Luttinger-liquid behavior and superconducting correlations in *t-J* ladders

C. A. Hayward and D. Poilblanc
Laboratoire de Physique Quantique, Université Paul Sabatier, 31062 Toulouse, France
(Received 19 September 1995)

The low-energy behavior of the isotropic *t-J* ladder system is investigated using exact diagonalization techniques, specifically finding the Drude weight, the charge velocity, and the compressibility. By applying the ideas of Luttinger-liquid theory, we determine the correlation exponent K_ρ which defines the behavior of the long-range correlations in the system. The boundary to phase separation is determined and a phase diagram is presented. At low electron density, a Tomonaga-Luttinger-like phase is stabilized while at higher electron densities a gapped phase with power law pairing correlations is stabilized: A large region of this gapped phase is found to exhibit dominant superconducting correlations.

I. INTRODUCTION

Over the last few years, the behavior of strongly correlated electrons confined to coupled chains has received widespread attention; the reasons for this are numerous. First, the behavior of electrons in one dimension, under *t-J* or Hubbard-type interactions, is now relatively well understood and described generally by the term Luttinger liquid (LL). The coupling of two such Luttinger liquids as in the ladder geometry provides an interesting first step towards the challenge of describing the behavior in two-dimensional systems. A second reason for interest in these systems lies in the unusual nature of the ground state in the undoped system, namely, spin liquid behavior with a finite gap in the spin excitation spectrum;[1] this behavior is in contrast to the gapless behavior of a single chain. The evolution of the spin-gapped state on doping has obvious relevance to gapped superconducting behavior. In addition, compounds such as $(VO_2)P_2O_7$ (Ref. 2) and $SrCu_2O_3$ (Ref. 3) are believed to be well described by a lattice of coupled chains. Very recently, experiments on $La_{1-x}Sr_xCuO_{2.5}$ (Ref. 4) have provided insight into the doping of coupled chain systems. While there is considerable literature on many aspects of the *t-J* ladder behavior, a complete picture is still far from being realized: Our aim in this paper is to clarify some of the behavior of the *t-J* ladder system by drawing on some of the ideas used in describing the strictly one-dimensional systems (i.e., LL theory). In conjunction with results from several other techniques, we will then present a speculative phase diagram.

The *t-J* Hamiltonian on the $2\times L$ ladder is defined as

$$\mathcal{H}=J'\sum_j (\mathbf{S}_{j,1}\cdot\mathbf{S}_{j,2}-\tfrac{1}{4}n_{j,1}n_{j,2})+J\sum_{\beta,j}(\mathbf{S}_{j,\beta}\cdot\mathbf{S}_{j+1,\beta}-\tfrac{1}{4}n_{j,\beta}n_{j+1,\beta})-t\sum_{j,\beta,s}P_G(c^\dagger_{j,\beta;s}c_{j+1,\beta;s}+\text{H.c.})P_G-t'\sum_{j,s}P_G(c^\dagger_{j,1;s}c_{j,2;s}+\text{H.c.})P_G, \quad (1)$$

where most notations are standard. β (=1,2) labels the two legs of the ladder (oriented along the x axis) while j is a rung index ($j=1,\ldots,L$). We shall concentrate on the isotropic case where the intraladder (along x) couplings J and t are equal to the interladder (along y) couplings J' and t'.

At half filling the Hamiltonian reduces to the Heisenberg model and the behavior is generally relatively well understood.[1] A simple interpretation is given by considering the strong coupling limit ($J=0$) in which the ground state consists of a singlet on each rung with a spin gap ($\sim J'$) which corresponds to forming a triplet on one of the rungs. With the introduction of intrachain coupling J, the triplets can propagate and form a coherent band, thereby reducing the spin-gap. In the isotropic case, the spin gap remains ($\sim 0.5J$).

The evolution of this spin-gapped state on doping is perhaps one of the most interesting aspects of the ladder behavior.[5] Recent work on this hole-doped phase[8,9,16] has indicated a finite spin gap, a single gapless charge mode, hole pairing, and possible dominant superconducting correlations. In this paper we shall discuss some independent results which provide a more complete description of not only this gapped phase but the whole region of parameter space. A possible phase diagram for the isotropic *t-J* ladder as a function of J/t and doping has been proposed recently[8] and we use these ideas in our analysis: Away from half filling the spin-gapped phase is stabilized up to $J/t\sim 2.1$ where the system phase separates.[10] As the system is doped further, a phase with a single gapless spin and a single gapless charge mode is found and, as we shall explain, this behavior is like that of the one-dimensional Tomonaga–Luttinger-liquid system. As in the gapped phase, phase separation occurs for large J/t. At very small electron densities, an electron-paired phase exists. Note that although in the *t-J* ladder there are four possible zero-momentum gapless modes (two spin and two charge), throughout the phase diagram only one gapless charge mode and either zero or one gapless spin mode are observed; this then allows an almost identical treatment to the strictly one-dimensional case.

In Sec. II we discuss briefly the Luttinger-liquid theory used to describe strictly one-dimensional systems and also the possible application of this theory to coupled chains, in Sec. III we present our numerical calculations, and finally in Sec. IV we apply the Luttinger-liquid theory to our results and present a phase diagram for the system.

 © 1996 The American Physical Society

II. LUTTINGER-LIQUID BEHAVIOR: TOMONAGA-LUTTINGER AND LUTHER-EMERY PHASES

In dealing with strictly one-dimensional interacting fermion systems, one can in general make use of conformal field theory[11] and bosonization[12] which allow a determination of the decay exponents of the various correlation functions to be determined from the low-energy behavior of the model. The general idea is that one-dimensional interacting fermion systems can be mapped onto the Fermi-gas model and the corresponding ''g-ology'' weak coupling theory.[13] This Fermi-gas model scales to two different regimes, namely, the Tomonaga-Luttinger (TL) fixed point and the Luther-Emery (LE) line which are relevant for repulsive ($g_1>0$) and attractive ($g_1<0$) backscattering matrix elements, respectively; as we shall explain, the important difference between these two universality classes lies in the spin degrees of freedom. The low-lying excitations of the Fermi-gas model are collective spin or charge density oscillations, which propagate with different velocities, giving rise to spin-charge separation and power law behavior of the correlation functions. In the TL phase, both a gapless spin and a gapless charge mode are exhibited; in contrast, while exhibiting a gapless charge mode, the LE phase has a gap to all spin excitations.

Conformal field theory relates the properties of a finite system (such as the compressibility and the Drude weight) with the correlation exponents; one coefficient (K_ρ) determines the exponents of all the power law decays (and similarly the singularity of the momentum distribution function close to k_f). Hence if a particular model scales to the TL (or LE) universality class, one can infer the dominant correlations from the low-energy behavior of the system which can be deduced from much smaller system sizes than would be required to calculate the correlation lengths directly.

The relationships between the correlation exponent (K_ρ) and the low-energy behavior of the model are given below for a system of size N and length L (we have chosen to give general equations such that $N=L$ for a chain, $N=2L$ for the ladder geometry). First, the ratio of the charge velocity u_ρ to the coefficient K_ρ is proportional to the variation of the ground state energy E_0 with particle density n, i.e., the inverse compressibility

$$\frac{\pi}{2}\frac{u_\rho}{K_\rho}=\frac{1}{n^2\kappa}=\frac{\partial^2(E_0/N)}{\partial n^2}. \tag{2}$$

The coefficient K_ρ is also related to the Drude weight σ_0; this Drude weight is the weight of the zero-frequency (dc) peak in the conductivity σ_ω and may be obtained by considering the curvature of the ground state energy level as a function of threaded flux, Φ,

$$\sigma_0=2u_\rho K_\rho=\frac{L^2}{4\pi}\frac{\partial^2(E_0/N)}{\partial\Phi^2}. \tag{3}$$

We can also determine the charge velocity by considering the dispersion of the energy spectrum

$$u_\rho=(E_{1\rho}-E_0)/(2\pi/L), \tag{4}$$

where $E_{1\rho}$ is the lowest-lying charge mode to the ground state (E_0) with neighboring k value.

TABLE I. Correlation exponents for the Tomonaga-Luttinger and Luther-Emery cases with $t'=0$. SS and TS indicate singlet and triplet superconductivity (pairing) correlations, respectively.

Correlation	TL	LE
$2k_f$ SDW	$1+K_\rho$	exponential
$2k_f$ CDW	$1+K_\rho$	K_ρ
SS	$1+1/K_\rho$	$1/K_\rho$
TS	$1+1/K_\rho$	exponential
$4k_f$ CDW	$4K_\rho$	$4K_\rho$

These equations provide us with three independent conditions on K_ρ and u_ρ which can be used to check the consistency of the Luttinger-liquid relations. Also a calculation of the parameter K_ρ is relatively straightforward and this parameter then determines the exponent coefficients of all the correlation functions.

As explained previously, the essential difference between the TL and LE fixed points lies in the spin degrees of freedom: The LE region is gapped while the TL region is gapless. For the one-dimensional case ($t'=0$) the correlation exponents of the two different cases are summarized in Table I (taken from Ref. 6). We have omitted the logarithmic corrections and these are detailed in Ref. 14. We emphasise that for LL systems, the correlation functions show either power law or exponential decay, with interaction-dependent powers determined by one coefficient K_ρ. Also we see that for $K_\rho<1$ (spin or charge) density waves (SDW, CDW) at $2k_f$ are enhanced and diverge, whereas for $K_\rho>1$ pairing fluctuations dominate.

While in strictly one-dimensional systems there is a single gapless charge mode, the theory could equally well be applied in a case where more than one gapless mode existed if the excitations were decoupled in the low-energy regime. In such a case, each degree of freedom would have an associated operator algebra, i.e., an associated K_ρ.

Specifically considering the problem of coupled chains, we note that at present little is known and there is much interest in how to connect the quasi-one-dimensional results to the strictly one-dimensional case. A recent calculation by Schulz[15] has considered the coupling of two Luttinger liquids by a small interchain hopping using a bosonization technique. Interestingly, in the presence of both forward and backward scattering terms, the calculation predicts a gap in all the magnetic excitations and a gapless charge mode (as observed for the hole-doped region of the t-J ladder). This gapped phase, however, exhibits somewhat different correlations to the strictly one-dimensional LE phase described above. First, the CDW_π and SDW_π correlations decay ex-

TABLE II. Correlation exponents for the spin gapped and gapless phases in the ladder geometry ($t'=t$). The π indicates that the correlations along the two chains are out of phase.

Correlation	Gapless	Gapped spin
$2k_f$ SDW_π	$1+2K_\rho$	exponential
$2k_f$ CDW_π	$1+2K_\rho$	exponential
SCd	$1+1/2K_\rho$	$1/2K_\rho$
$4k_f$ CDW	$8K_\rho$	$2K_\rho$

ponentially along the chains (we use the notation of Schulz where 0 or π indicate the oscillations are in or out of phase between the two chains, respectively, i.e., ''bonding'' or ''antibonding''). A divergent density-density response, decaying as $\sim\cos[2(k_f^0+k_f^\pi)r]r^{-2K_\rho}$, exists in analogy with the $4k_f$ oscillations of a single chain (k_f^0 and k_f^π refer to the Fermi points of the bonding and antibonding quasiparticle branches, respectively); the definition of K_ρ is the same as that used previously for the strictly one-dimensional case. The superconducting correlations (cross chain pairing) decay as $r^{-1/2K_\rho}$ and exhibit a d-like character. Hence for this gapped phase, we would expect dominant superconducting correlations for $K_\rho>1/2$. In agreement with these findings, different approaches by Troyer *et al.*,[16] Nagaosa,[17] and Balents and Fisher[18] predict similar behavior in the spin-gapped region, i.e., Luther-Emery-like in the sense that there exist two order parameters (analogous to the on-site pairing and $2k_f$ CDW in the LE class) whose exponents obey a reciprocal relation: These correspond to the pair field correlations and to a four-fermion operator $\langle n_B(r)n_B(0)\rangle$, where n_B is the density of ''bosonic'' hole pairs bound on a rung [analogous to the $4k_f$ oscillations of a single chain (i.e., $2k_f^0+2k_f^\pi$)]. In Table II we summarize the correlation exponents predicted for the case where $t=t'$, i.e., the ladder geometry. Note that in electing to retain the previous definition of K_ρ, the exponents of the gapless ''TL'' phase are rescaled ($K_\rho\mapsto 2K_\rho$).

In the following section we give details of calculations using these ideas to characterize the behavior of the t-J ladder, finding the parameter K_ρ and hence the dominant correlation functions. We consider various electron densities and various ratios of J/t to build up a speculative phase diagram.

III. NUMERICAL CALCULATIONS

Since we require information concerning the low-energy properties of the model, the dominant technique we have employed is that of exact diagonalization of finite systems, specifically 2×5 and 2×10 double chain rings. Exact diagonalization techniques are particularly well adapted to the investigation of low-energy modes since implementation of various quantum numbers is straightforward; the various excitation modes can be obtained by calculating the ground state energy in each symmetry sector. The low-energy modes of the system are characterized first by their spin: Singlet and triplet excitations correspond to charge and spin modes, respectively. It is also useful to consider the parity of the states under a reflection in the symmetry axis of the ladder along the direction of the chains: Even ($R_x=1$) or odd ($R_x=-1$) excitations corresponding to bonding (B) or antibonding (A) modes, respectively (0 and π as used by Schulz[15]). Finally the dispersion relation of each mode is determined by the momentum $k_x=2\pi n/L$.

In order to ensure that the antiferromagnetic correlations are not frustrated when one goes around each chain, we have chosen the electron number to be always a multiple of 4; our results then concern electron densities 0.4 and 0.8 for both system sizes and in addition 0.2 and 0.6 for the larger system size. The absolute ground state is given by the boundary conditions that form a closed shell in the noninteracting Fermi sea (obtained by turning off the interaction J) and these are used in the calculations of u_ρ and κ, specifically antiperiodic boundary conditions for $n<0.5$ and periodic boundary conditions for $n>0.5$.

A. Drude weight and anomalous flux quantization

The first calculation we present concerns the Drude weight, defined by Eq. (3). The numerical technique involves threading the double chain ring with a flux Φ and studying the functional form of the ground state energy with respect to the threaded flux, namely, $E_0(\Phi)$. In general $E_0(\Phi)$ consists of a series of parabolas, corresponding to the curves of the individual many-body states $E_n(\Phi)$: This envelope exhibits a periodicity of 1, where we have chosen to measure the flux in units of the flux quantum $\Phi_0=hc/e$. Note that the function $E_0(\Phi)$ also gives a quantitative value of the superfluid density D_s, which is in general different from σ_0.[19] The Drude weight corresponds to curvature of a single ground-state many-body energy level while the superfluid density corresponds to the curvature of the envelope of the individual many-body states as a function of flux. However, since the flux (ϕ_c) at which another many-body energy level crosses the zero-flux ground state energy level varies as $\phi_c\sim(hc/e)L^{1-d}$ (where d is the dimension),[19] in one dimension ϕ_c is independent of L; there is only a finite number of energy level crossings in the thermodynamic limit and σ_0 and D_s are equal (up to a factor of 2π).

In addition to the Drude weight and the superfluid density, the function $E_0(\Phi)$ also yields information regarding the phenomenon of anomalous flux quantization; this has been explained in a previous publication,[9] and so we mention it only briefly here. While in general the ground state envelope $E_0(\Phi)$ exhibits a periodicity of 1, Byers and Yang[20] have shown that in the thermodynamic limit $E_0(\Phi)$ exhibits local minima at quantized values of flux, the separation of which is $1/n$ where n is the sum of the charges in the basic group. Hence, for a paired superconducting state we would expect minima in $E_0(\Phi)$ at intervals of 1/2. These minima are related to the existence of supercurrents which are trapped in metastable states corresponding to the flux minima and are thus unable to decay away.[21] It should be mentioned that this anomalous flux quantization (AFQ) is an indication of pairing and is not in itself sufficient to imply a superconducting state.

Numerically the application of a flux through the double-chain ring is achieved by modifying the kinetic term of the Hamiltonian such that

$$c^\dagger_{j,\beta;s}c_{j+1,\beta;s}\mapsto c^\dagger_{j,\beta;s}c_{j+1,\beta;s}e^{i2\pi\Phi/L}, \tag{5}$$

where Φ is the flux through the ring measured in units of Φ_0. Hence the application of a flux is numerically equivalent to a change in the boundary conditions of the problem, $\Phi=0$ representing periodic and $\Phi=1/2$ representing antiperiodic boundary conditions. In the thermodynamic limit, σ_0 must be independent of the phase introduced at the ring boundary[22] and therefore we consider the whole of the envelope $E_0(\Phi)$ as a function of flux (in general consisting of several parabolas).

Choosing the parameters $n=0.8$ and $J/t=0.5$, we show in Fig. 1(a) [1(b)] all the possible spin and charge modes of the 2×5 [2×10] system, for all possible momenta, as a

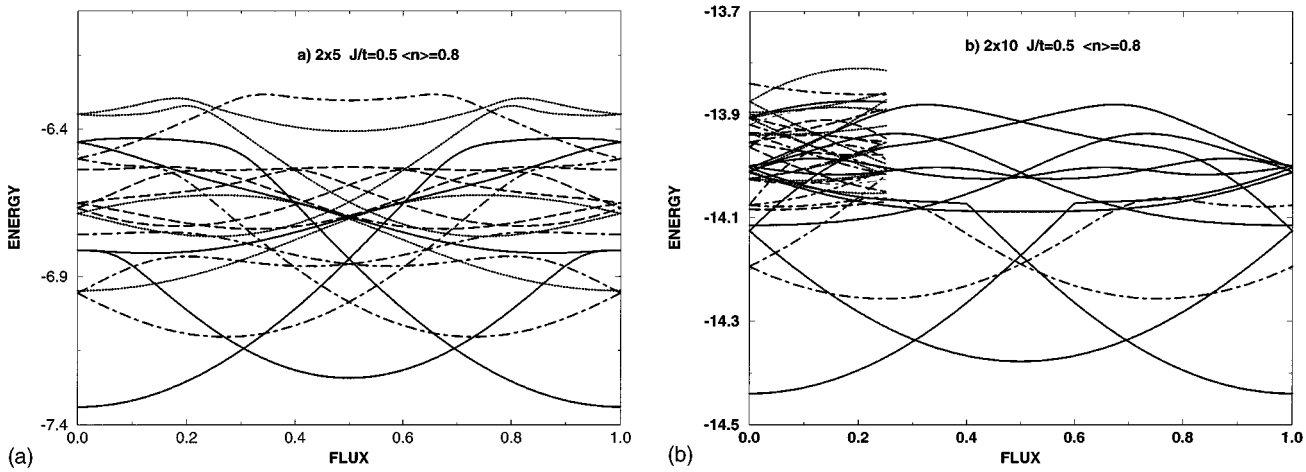

FIG. 1. Energy as a function of flux (in units of $\Phi_0 = hc/e$) for (a) the 2×5 and (b) the 2×10 ladders with $J/t=0.5$ and $n=0.8$. We show all possible momenta for various quantum numbers: For the charge modes, the solid lines correspond to bonding and the dotted lines to antibonding, while for the spin modes the dashed lines correspond to bonding and the dot-dashed lines to antibonding. For the larger system size, we give only the charge bonding and the lowest-lying spin antibonding mode in full to simplify the diagram.

function of applied flux. In the case of the larger system, we show the full spectrum for $\Phi<0.25$ in order to simplify the diagram (this work has been previously published[9]). For both system sizes the minimum energy is formed by charge (spin zero) bonding modes; the excited modes with different quantum numbers move farther from the ground state as the system size is increased (a result we have checked by finite-size scaling) and hence will not interfere with $E_0(\Phi)$. The existence of minima at intervals of half a flux quantum (i.e., anomalous flux quantization) clearly indicates the existence of pairing.

The envelope $L[E_0(\Phi)-E_0(\Phi=0)]$ has been extracted and is shown in Figs. 2(a) and 2(b) along with equivalent plots from other regions of the phase diagram: Figure 2(a) shows the data for $J/t=1.0$ and electron densities of 0.4 and 0.8, while Fig. 2(b) shows the data for an electron density of 0.8 for ratios $J/t=0.5$ and 4.0. Apart from the curve with $n=0.8$, $J/t=4.0$ (which appears to scale to a flat function, consistent with a phase-separated state), all the data appear to show only small finite-size effects. Anomalous flux quantization is observed for the larger electron density (for the lower values of J/t), indicating pairing, and hence consistent with a superfluid state in this region.

In order to determine the Drude weight, we simply calculate the average value of the curvature of $L[E_0(\Phi)-E_0(\Phi=0)]$ over all Φ; a quadratic curve was fitted to each portion. In Fig. 3(a) we plot the Drude weight as a function of J/t for electron densities 0.2, 0.4, 0.6, and 0.8 for the 2×10 system and electron densities 0.4 and 0.8 for the 2×5 system. The curves are plotted up to a maximum in J/t which is determined by the value at which the system phase separates (see compressibility). In Fig. 3(b) we plot the Drude weight as a function of electron density for various values of the ratio J/t.

There are several features of the resulting behavior we should mention: Note first that finite-size effects are relatively small with the 2×5 results close to those of the 2×10 results. The Drude weight increases as the electron

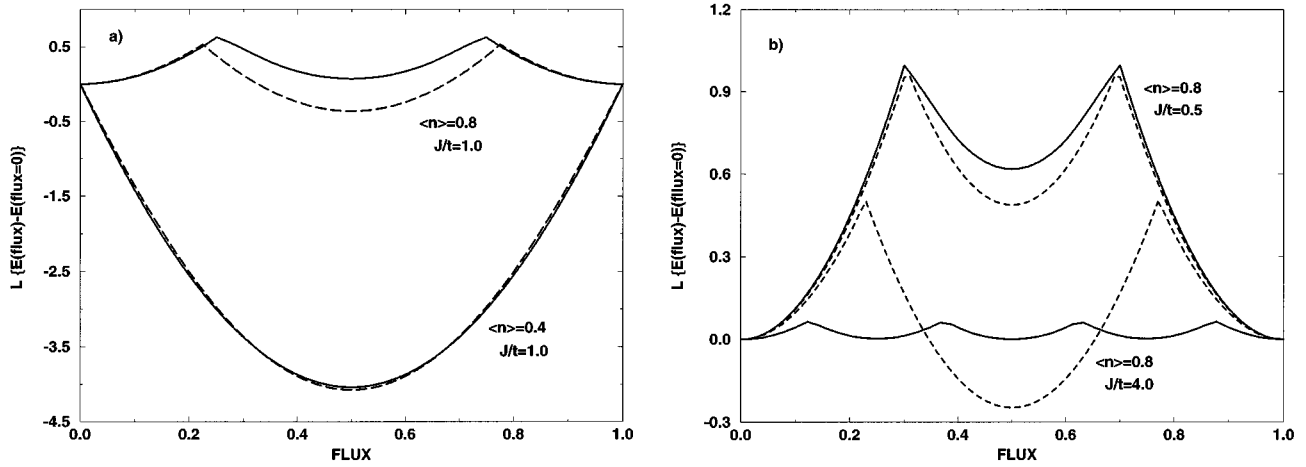

FIG. 2. $L[E_0(\Phi)-E_0(\Phi=0)]$ where L is the length of the ladder and $E_0(\Phi)$ is the ground state energy with an applied flux Φ. The dashed lines correspond to 2×5, the solid lines to 2×10. (a) shows the results for $n=0.4$ and $n=0.8$ both with $J/t=1.0$, while (b) shows $J/t=0.5$ and $J/t=4.0$ both with $n=0.8$.

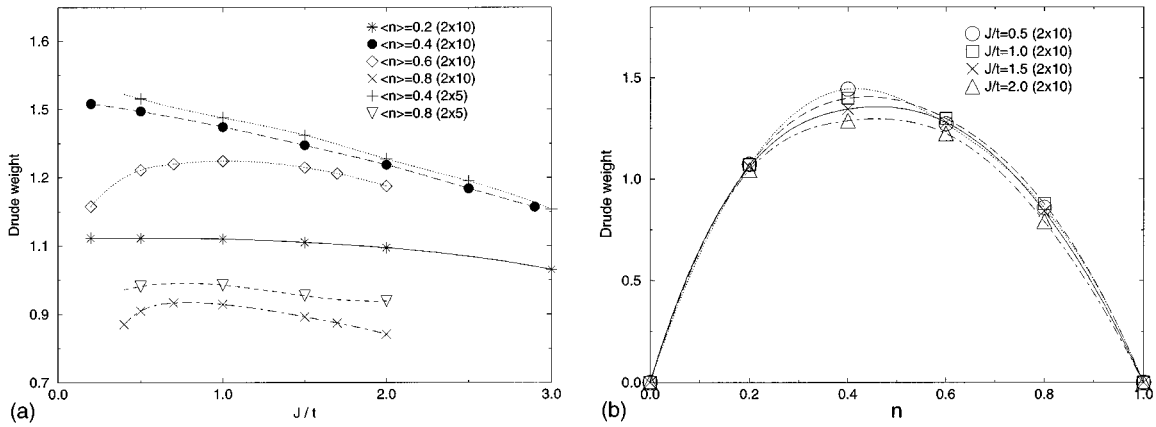

FIG. 3. The Drude weight σ_0 (a) as a function of ratio J/t for various electron densities and system sizes, and (b) as a function of electron density for various J/t. The solid lines are a guide to the eye.

density is increased from zero, until it reaches one-quarter filling, and then decreases with increasing electron density. Also, as we would expect for a spin-charge-separated state, the Drude weight is effectively independent of J.

B. Charge velocity

The second quantity we have calculated is the charge velocity, defined by Eq. (4). Considering the charge bonding modes (the lowest-lying charge modes), the energy difference between the ground state energy level and the energy level with neighboring momentum, $\Delta k_x = 2\pi/L$ was calculated. As an example, we show in Fig. 4(a) the charge bonding modes for the case $n=0.4$, $J/t=2.0$, indicating with solid lines the specific energy levels whose energy difference gives the charge velocity. We note that the gap (and therefore u_ρ) is approximately constant as a function of flux. For consistency with future data, however, we have calculated the charge velocity at the particular flux which gives the absolute ground state, i.e., $\Phi=0.5$ for $n<0.5$ and $\Phi=0$ for $n>0.5$; the results are shown in Fig. 4(b) as a function of J/t for various system sizes and various electron densities (the results for $n=0.6$ are not included since the numerics present some difficulty close to one-quarter filling). Note again that finite-size effects are relatively small.

C. Compressibility

The next quantity we calculate is that of the compressibility, defined by Eq. (2). The finite-size equivalent is given by

$$\frac{1}{n^2\kappa} \simeq \frac{1}{2L}\left[\frac{E_0(n+\Delta n)+E_0(n-\Delta n)-2E_0(n)}{(\Delta n)^2}\right], \quad (6)$$

where $E_0(n)$ is the ground state energy of the finite system of ladder length L with an electron density n. As for the calculation of the charge velocity, the boundary conditions have been chosen to give the absolute ground state. Δn represents the finite change in electron density, 0.2 and 0.4 for the 2×10 and 2×5 systems, respectively. In Fig. 5 we show the results of the calculation of $1/n^2\kappa$ for electron densities corresponding to 0.2, 0.4, 0.6, and 0.8 for the 2×10 ladder and we also plot the result of the 2×5 system for an electron density of 0.4.

In addition to the determination of the specific values of the inverse compressibility, the boundary to phase separation may also be determined from these results. It is well known

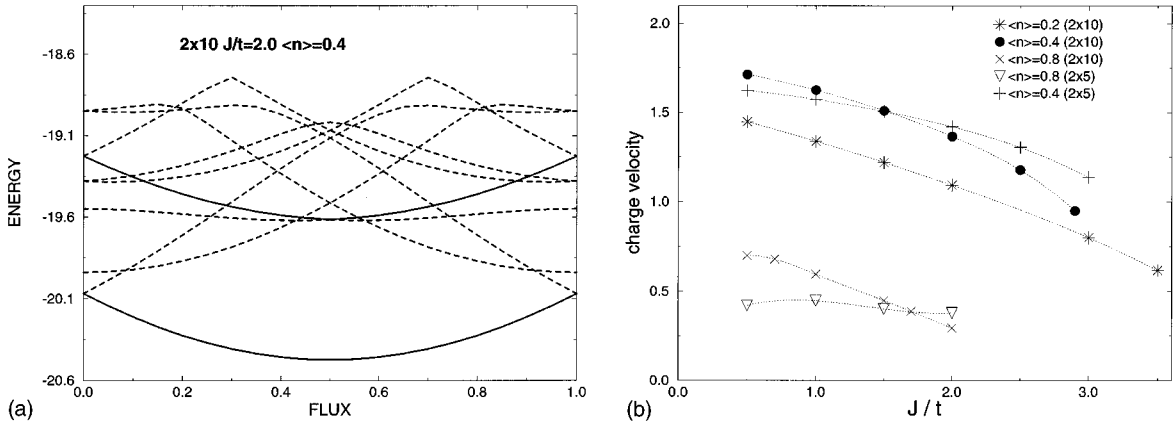

FIG. 4. (a) Energy of the charge bonding modes as a function of flux for the 2×10 system with $n=0.4$, $J/t=2.0$. The solid lines indicate the ground state and the excited states used to calculate the charge velocity. (b) The charge velocity u_ρ as a function of ratio J/t for various electron densities and system sizes. The dotted lines are a guide to the eye.

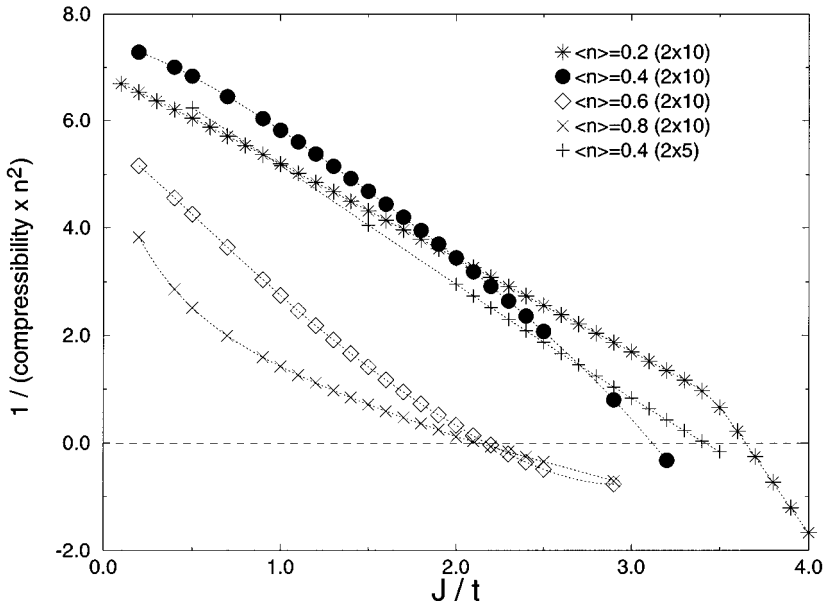

FIG. 5. $1/n^2\kappa$ as a function of ratio J/t for various electron densities and system sizes. The dotted lines are a guide to the eye.

that at sufficiently large values of J/t, a system will undergo a separation into two phases, a hole-rich and an electron rich phase. This effect arises principally to minimize the number of broken antiferromagnetic bonds in the system. Phase separation occurs when the compressibility diverges (i.e., a ''liquid'' to a ''solid'' phase) and hence the inverse compressibility vanishes. While there remain some small finite-size effects, the general form of the phase separation line is readily observed from Fig. 5. As electron density is increased, the value of J/t at which phase separation occurs decreases (although electron densities of 0.6 and 0.8 both indicate phase separation close to $J/t \sim 2.1$). These results agree well with those of Tsunetsugu *et al.*[10] who used a similar technique but varied both system size and electron density simultaneously. The phase separation curve can be extrapolated to all electron densities and will be shown in the predicted phase diagram, Fig. 8.

IV. LUTTINGER-LIQUID PARAMETERS FOR THE LADDER

In order to explore the validity of the Luttinger-liquid relations in our problem, we consider the ratio $\sigma_0/\pi n^2\kappa u_\rho^2$ which equals unity for a Luttinger liquid. The results of the numerical calculation of this quantity are shown in Fig. 6 for various electron densities.

At low electron densities (i.e., for the cases $n=0.2$ and $n=0.4$), previous work has suggested that a TL phase is stabilized and the results of this ratio show good agreement with the predicted value of unity; for the case of $n=0.4$ an increase in system size shows the ratio scaling towards unity. For the hole-doped spin-gapped region ($n=0.8$), where the behavior is less well understood, the system phase separates at a much lower value of J/t and hence the curve drops to zero at $J/t \sim 2.1$. Before this phase separation, the data are not inconsistent with the LE-like behavior which may be

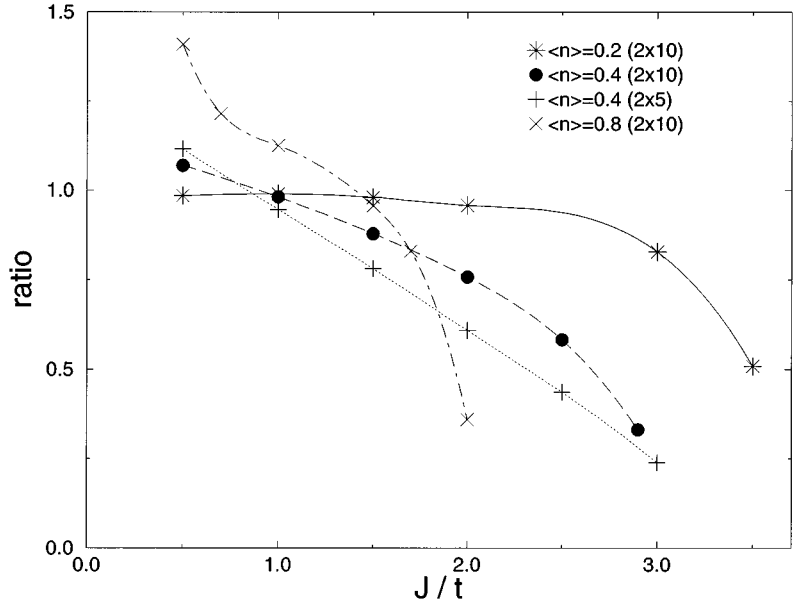

FIG. 6. The ratio $\pi n^2\kappa u_\rho^2/\sigma_0$ as a function of J/t for various electron densities and system sizes. The dotted lines are a guide to the eye.

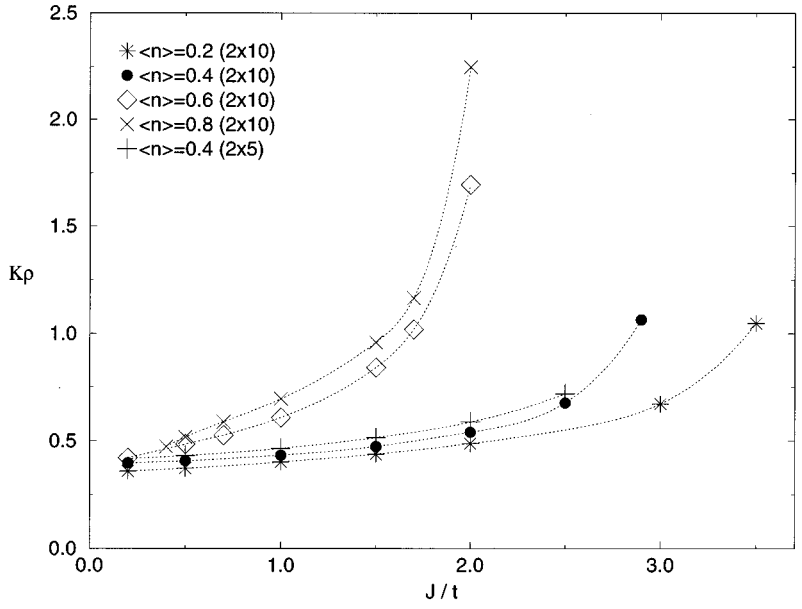

FIG. 7. K_ρ as a function of ratio J/t for various electron densities and system sizes. The dotted lines are a guide to the eye.

described by Eqs. (2)–(4) (finite-size effects are largest for high electron density and low J/t). Since the ratio is close to unity, it appears to confirm the earlier justification for using this one-dimensional theory; i.e., only a single gapless charge mode is observed.

With the values of the compressibility and the Drude weight, we can obtain an estimate of the coefficient K_ρ using $K_\rho = 1/2\sqrt{\pi n^2 \kappa \sigma_0}$. This behavior of K_ρ for the different electron densities of the 2×10 ladder is shown in Fig. 7 and we have also plotted the results for a 2×5 ladder with electron density 0.4. Note that as J/t is increased, K_ρ increases (for all electron densities), becoming infinite at phase separation as the compressibility diverges. A similar calculation has been performed by Troyer and co-workers[16,10] for a specific electron density of 0.857, i.e., two holes on a 2×7 ladder, and the results are consistent in this region.

Before analyzing the behavior further, specifically the importance of K_ρ, we present a speculative phase diagram of the isotropic t-J ladder as a function of J/t and electron density. This phase diagram is shown in Fig. 8 and we discuss briefly the various regions.

At larger values of J/t, the system phase separates, and to estimate the value of J/t at which this occurs, we show the data points at which the inverse compressibility vanishes in the 2×10 system (see Fig. 5). On doping away from half filling, the spin gap region persists and a phase exhibiting one gapless charge mode is stabilized. On further doping a gapless phase is stabilized: The schematic boundary between these two phases is shown as a dot-dashed line. As for both the one- and two- dimensional t-J cases,[24] a gas of electron

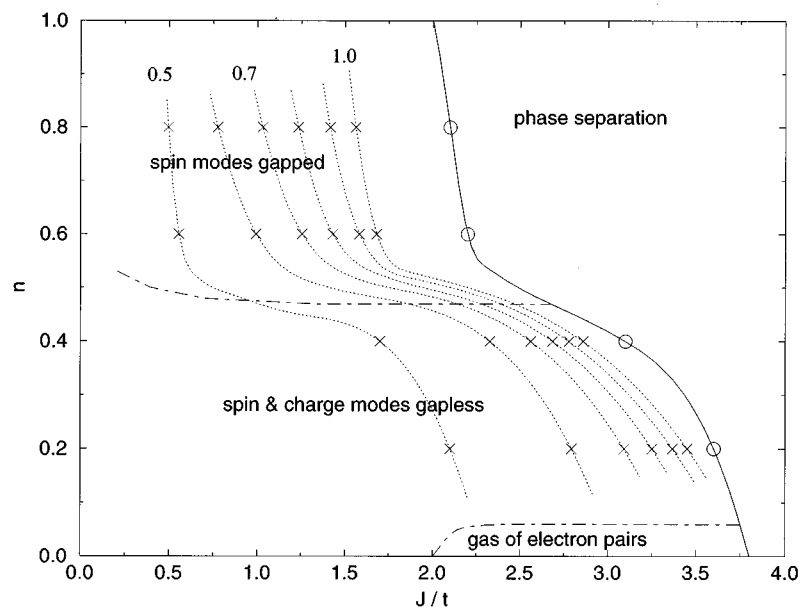

FIG. 8. Speculative phase diagram of the t-J ladder as a function of J/t and electron density n. The circles and crosses represent results from the 2×10 system and the dotted lines are guides to the eye. The dot-dashed lines separating the different phases are estimated.

pairs is formed at low electron densities above a critical value of the ratio J/t; other $2p$-particle ($p>1$) bound states could also become stable at larger J/t in this region. Again the boundary to this paired phase is shown as a dot-dashed line and is schematic.

From the data in Fig. 7 we have plotted contours of constant K_ρ in order to allow a determination of the dominant correlation functions. While the parameter K_ρ is continuous for a particular value of J/t as the electron density is varied,[23] at some region between $n=0.4$ and $n=0.8$ a gap opens in the spin excitation spectrum and the correlation functions change their form discontinuously, scaling to a different fixed point as explained in Sec. II. A ''jump'' in the exponent of the superconducting correlations occurs with the SCd charge exponent changing from $1+1/2K_\rho$ to $1/2K_\rho$; the $2k_f$ CDW correlations jump from power law behavior (exponent $1+2K_\rho$) to exponential decay. In addition, in the gapped high-density state we would expect conjugate ''four fermion $4k_f$'' CDW correlations with exponent $2K_\rho$.

For both the high-density gapped phase and the low-density TL phase we expect different correlation functions to dominate either side of the contour $K_\rho=1/2$; in both cases superconducting correlations dominate for $K_\rho>1/2$. However, in the gapped hole-doped phase, this region is much larger and, in contrast to other models such as the one-dimensional t-J model,[24] does not just exist as a precursor to phase separation. A physical picture of the behavior is of the holes pairing up on the rungs, the spins in singlets, and the dominant correlation functions are then associated with the movement of the hole pairs.

ACKNOWLEDGMENTS

We wish to thank H.J. Schulz for many useful discussions and comments; we also gratefully acknowledge many helpful conversations with M. Luchini, F. Mila, W. Hanke, and D.J. Scalapino. Laboratoire de Physique Quantique, Toulouse is Unité de Recherche Associé au CNRS No 505. C.A.H. and D.P. acknowledge support from the EEC Human Capital and Mobility program under Grant Nos. ERBCHBICT941392 and CHRX-CT93-0332. We also thank IDRIS (Orsay) for allocation of CPU time on the C94 and C98 CRAY supercomputers.

[1] T. Barnes *et al.*, Phys. Rev. B **47**, 3196 (1993); S. Gopalan, T. M. Rice, and M. Sigrist, *ibid.* **49**, 8901 (1994).
[2] D.C. Johnston *et al.*, Phys. Rev. B **35**, 219 (1987).
[3] Z. Hiroi *et al.*, Physica C **185-189**, 523 (1991); M. Takano *et al.*, Jpn. J. Appl. Phys. **7**, 3 (1992).
[4] Z. Hiroi and M. Takano, Nature **397**, 41 (1995).
[5] The effect of doping spin gapped systems and the possible presence of superconducting correlations has been studied previously in various one-dimensional models, e.g., t-J-J' Hamiltonian (Ref. 6) and the dimerized t-J model (Ref. 7).
[6] M. Ogata *et al.*, Phys. Rev. B **44**, 12 083 (1991).
[7] M. Imada, Phys. Rev. B **48**, 550 (1993).
[8] D. Poilblanc, D.J. Scalapino, and W. Hanke, Phys. Rev. B **52**, 6796 (1995).
[9] C.A. Hayward, D. Poilblanc, R.M. Noack, D.J. Scalapino, and W. Hanke, Phys. Rev. Lett. **75**, 926 (1995).
[10] H. Tsunetsugu, M. Troyer, and T.M. Rice, Phys. Rev. B **51**, 16 456 (1995).
[11] N. Kawakami and S.K. Yang, Phys. Rev. Lett. **65**, 2309 (1990).
[12] H.J. Schulz, Phys. Rev. Lett. **64**, 2831 (1990).
[13] J. Solyom, Adv. Phys. **28**, 209 (1979); V.J. Emery, in *Highly Conducting One-Dimensional Solids*, edited by J.T. Devreese *et al.* (Plenum, New York, 1979), p. 327.
[14] T. Giamarchi and H.J. Schulz, Phys. Rev. B **39**, 4620 (1989).
[15] H.J. Schulz (unpublished).
[16] H. Tsunetsugu, M. Troyer, and T. M. Rice, Phys. Rev. B **49**, 16 078 (1994); **51**, 16 456 (1995).
[17] N. Nagaosa (unpublished).
[18] L. Balents and P.A. Fisher (unpublished).
[19] D.J. Scalapino, S.R. White, and S. Zhang, Phys. Rev. B **47**, 7995 (1993).
[20] N. Byers and C.N. Yang, Phys. Rev. Lett. **7**, 46 (1961).
[21] J.R. Schrieffer, *Theory of Superconductivity* (Benjamin, New York, 1964).
[22] R.M. Fye *et al.*, Phys. Rev. B **44**, 6909 (1991).
[23] M. Troyer *et al.*, Phys. Rev. B **48**, 4002 (1993).
[24] M. Ogata *et al.*, Phys. Rev. Lett. **66**, 2388 (1991).